*Proceedings of the 21st ICSMGE, Vienna, Austria, 14 – 19 June 2026. Pistrol, Adam & Schweiger (eds.)*
*Published by: ÖGG, Austrian Society for Geomechanics, Salzburg, Austria, ISBN 978-3-9503898-4-5*
*https://doi.org/10.53243/ICSMGE2026-1355*

# Numerical Simulation of $CO_2$ Injection and Hydrate Formation in Marine Sediment

**Chea Sokpheanika,** Park Changhee, Kim Jin, Cho Gye-Chun
*Department of Civil and Environmental Engineering, Korea Advanced Institute of Science and Technology (KAIST), Daejeon, Republic of Korea, gyechun@kaist.ac.kr*

ABSTRACT: Geological carbon dioxide storage (GCS) through hydrate formation in marine sediments offers a promising approach to reducing atmospheric $CO_2$ emissions while maintaining environmental stability. When $CO_2$ is injected into sub-seafloor sediments, gas hydrates can form at the interface of $CO_2$ and brine under specific pressure-temperature (P-T) conditions. This study presents a numerical simulation of the coupled processes of $CO_2$ injection, hydrate formation, and fluid displacement in porous marine sediments. The primary aim is to evaluate the feasibility of $CO_2$ hydrate formation and its impact on local P-T conditions and hydrate formation rates. A modified kinetic model incorporating a thermal energy balance equation accounts for the exothermic heat released during hydrate formation, which influences local P-T behavior. Numerical simulations conducted in COMSOL Multiphysics focus on key parameters, including injection rate, sediment temperature, and pressure. The results show continuous gas hydrate formation over time, with a maximum $CO_2$ conversion efficiency of 87.4% by the end of the simulation. Initially, hydrate formation causes localized temperature increases due to exothermic reactions, while pressure rises steadily near the injection point before gradually stabilizing as reduced permeability limits further fluid flow. These findings emphasize the need to carefully evaluate injection conditions and site characteristics to optimize hydrate-based carbon storage. Overall, the study confirms the viability of $CO_2$ storage through hydrate formation under favorable temperature and pressure conditions in ensuring successful and efficient carbon sequestration.

KEYWORDS: Gas hydrate, formation, $CO_2$ injection, carbon storage, COMSOL Multiphysics.

## 1 INTRODUCTION

Due to rapid industrialization, urbanization, and population growth, carbon dioxide ($CO_2$) emissions have increased to unprecedented levels. Globally, atmospheric $CO_2$ concentration has nearly reached 420 parts per million (ppm), a significant rise from the pre-industrial level of approximately 280 ppm (Méndez et al., 2023). This surge in $CO_2$ levels is a major driver of global warming and climate change.

In response, various $CO_2$ mitigation technologies have been proposed, including the use of recycled materials, renewable energy, nuclear fusion, and biofuels. Among these options, carbon capture and storage (CCS) stands out as one of the most effective and cost-efficient methods for rapidly reducing atmospheric $CO_2$ (Bachu, 2003). Unlike other mitigation strategies, CCS directly prevents $CO_2$ from being released back into the atmosphere, offering immediate climate benefits.

CCS is particularly well-suited for large-scale implementation due to the vast geological formations available for storage. Once injected, $CO_2$ can remain securely trapped for long periods, making CCS a sustainable long-term solution for carbon reduction. This process, known as carbon sequestration, involves capturing and storing $CO_2$ to enhance the Earth's natural carbon sinks (Keenan & Williams, 2018).

Carbon storage methods are generally categorized based on the physical state of $CO_2$: either in a supercritical fluid state or as a solid. Solid-state storage, specifically in the form of gas hydrate, is considered especially promising because it eliminates the risk of leakage. Moreover, the formation of $CO_2$ hydrates can increase the rigidity of surrounding soils, providing an added benefit for geotechnical stability (Zheng et al., 2020). Oceanic environmental conditions are highly favorable for gas hydrate formation. Moreover, the vast extent of the world's oceans makes this method particularly attractive for large-scale applications. Figure 1 shows the $CO_2$ hydrate stability zone in a hypothetical oceanic location.

In the study, we aim to verify whether gas hydrates can actually form when $CO_2$ is injected into the saline aquifer. During $CO_2$ injection into cold saline aquifers, $CO_2$ hydrate can form at the interface of $CO_2$ and brine under specific temperature and pressure conditions. This chapter investigates a coupled $CO_2$ hydrate formation and displacement process through numerical simulations, focusing on how to hydrate formation influences the temperature and pressure of the domain and the connection between P-T and hydrate formation rate.

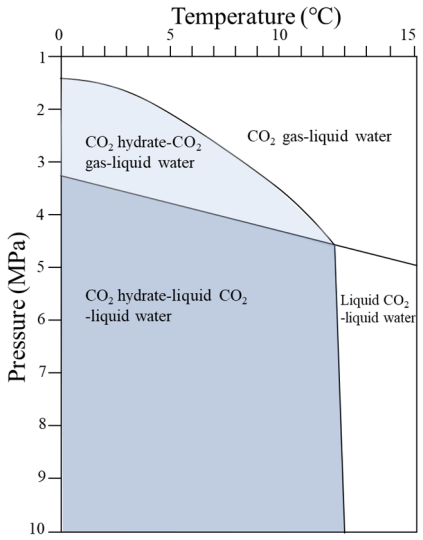


Figure 1. $CO_2$ hydrate stability zone in a hypothetical oceanic location

An improved kinetic hydrate formation model is used to achieve this, incorporating a thermal energy balance equation that accounts for the exothermic nature of hydrate formation and its effects on local temperature and pressure. Numerical simulations are performed using COMSOL Multiphysics to analyze the interactions between $CO_2$ injection and hydrate formation. The results demonstrate that $CO_2$ hydrate formation increases local pressure and temperature rise due to the exothermic reaction of hydrate formation lowers the hydrate formation rate.

## 2 NUMERICAL STUDY

### 2.1 *Candidate sites for simulation*

This study focuses on identifying areas in Korea's offshore sites, such as Ulleung Basin, Gunsan Basin, and Jeju Basin,

where pressure-temperature (P-T) conditions are suitable for forming and maintaining $CO_2$ hydrate.

### 2.2 *Problem statement*

The process of injecting supercritical $CO_2$ into porous saline aquifers involves the interaction of the $CO_2$ phase (non-wetting phase), the brine phase (wetting phase), and the displacement mechanism. When the displacing phase enters the formation through the injection well, the brine is gradually displaced, leading to interactions and transport between the two phases. During this displacement process, $CO_2$ moves through the porous media, sweeping areas containing residual brine. Under conditions of low temperature and high pressure, this interaction leads to the formation of $CO_2$ hydrate.

In this study, we integrate the two-phase displacement process with the hydrate formation process to explore the impact of hydrate formation on the $CO_2$ injection process and the displacement mechanism. To simplify the physical model, the following assumptions are made: (1) The saline aquifer is treated as a homogeneous porous medium. (2) $CO_2$ hydrate, brine, and $CO_2$ fluid are separate phases occupying the pore spaces. (3) In the saline aquifer, $CO_2$ and brine are immiscible phases, and the effect of mutual dissolution is disregarded. (4) The temperature gradient and hydrostatic pressure gradient are assumed to follow a linear distribution. (5) At the initial condition, the porous media contains only water, without any other impurity.

### 2.3 *Governing equations*

#### 2.3.1 *Gas-water flow model in porous media*

The gas-water two-phase flow resulting from hydrate decomposition in porous media can be described using the unsaturated Darcy multiphase flow theory, commonly employed in classical soil mechanics. This framework treats $CO_2$ as the non-wetting phase, while water is considered the wetting phase. This relationship is mathematically represented as follows (Deng et al., 2020):

$$v_i = -\frac{Kk_{r,i}}{\mu_i}(\nabla p_i - \rho_i g), \qquad i = g, w \tag{1}$$

$$\frac{\partial \varphi_{wg}\rho_i S_i}{\partial t} + \nabla \cdot \rho_i v_i = m_g, \qquad i = g, w \tag{2}$$

- $v_i$ represents the Darcy velocity, measured in $\mathrm{m/s}$.
- $\mu_i$ denotes the dynamic viscosity of the fluid in $\mathrm{Pa \cdot s}$.
- $K$ is the absolute permeability, measured in mD.
- $k_{r,i}$ is the relative permeability, dimensionless.
- $p_i$ represents the fluid pressure, measured in Pa.
- $g$ is the gravitational acceleration in $\mathrm{m/s^2}$.

Here, $k_{r,i}$ is the relative permeability of each phase, which is defined by the van Genuchten-Mualem (Chen et al., 1999):

$$k_{rw} = s_e^b[1 - \left(1 - s_e^{\frac{1}{a}}\right)^a]^2 \tag{3}$$

$$k_{rg} = (1 - s_e)^c(1 - s_e^{\frac{1}{a}})^{2a} \tag{4}$$

#### 2.3.2 *Thermal model in porous media*

Temperature plays a critical role in influencing hydrate formation. Hydrate formation occurs only when the temperature in the porous media falls below the hydrate phase equilibrium temperature under the given pressure conditions. Temperature distribution within porous media is dynamic and is influenced by heat transfer processes. These include heat conduction, convection, external heat supply, and the heat exchange associated with the hydrate phase transition.

Based on the principle of energy conservation and incorporating these heat transfer effects, a heat transfer model for porous media was developed to calculate the dynamic temperature distribution within the medium. This model allows for analyzing how temperature variations impact hydrate formation and stability, providing a foundation for understanding the thermal dynamics during gas-water interactions in hydrate-bearing formations (Deng et al., 2020).

$$(\rho C)_{eq}\frac{\partial T}{\partial t} + \left(\rho_g C_g v_g + \rho_w C_w v_w\right) \cdot \nabla T - \nabla \cdot (\lambda_{eq}\nabla T) = Q \tag{5}$$

In this Eq. (5), T represents the temperature in Kelvin (K), while t refers to the time in seconds (s). The parameters $\rho_g$ and $\rho_w$ denote the densities of gas and water, respectively, expressed in $\mathrm{kg/m^3}$. Similarly, $C_g$ and $C_w$ indicate the specific heat capacities of gas and water, measured in $\mathrm{J/(kg \cdot K)}$. The terms $v_g$ and $v_w$ represent the Darcy velocities of methane and water, respectively, with units of $\mathrm{m/s}$. Finally, $\lambda_{eq}$ stands for the equivalent heat transfer coefficient, expressed in $\mathrm{W/(m \cdot K)}$.

Gas, water, hydrate, and reservoir skeletons coexist within porous media, where the content of the reservoir skeleton remains constant. However, the volume fraction distributions of gas, water, and hydrate change dynamically with the gas-water two-phase flow and hydrate formation processes. Consequently, the heat transfer parameters in the above equation can be calculated using the volume fraction weighted average rule. This approach is applied to account for the contributions of each phase to the overall heat transfer, as expressed in the following formulas:

$$(\rho C)_{eq} = \varphi\rho_g S_g C_g + \varphi\rho_w S_w C_w + \varphi\rho_h S_h C_h + (1 - \varphi)\rho_s C_s \tag{6}$$

$$\lambda_{eq} = \varphi S_g \lambda_g + \varphi S_w \lambda_w + \varphi S_h \lambda_h + (1 - \varphi)\rho_s \lambda_s \tag{7}$$

where $\varphi$ is absolute porosity, dimensionless; $S_g$ $(i = g, w, h)$ is the saturation of gas, water, and hydrate, dimensionless; $\rho_h$ and $\rho_s$ are the density of hydrate and skeleton, respectively, $\mathrm{kg/m^3}$; $C_h$ and $C_s$ are specific heat capacity of hydrate and skeleton, $\mathrm{J/(kg \cdot K)}$. $\lambda_s(i = g, w, h)$ is the heat transfer coefficients of gas, water, and hydrate, $\mathrm{W/(m \cdot K)}$. $S_h$ is the hydrate saturation, dimensionless.

When the temperature and pressure conditions necessary for hydrate formation are met in porous media, the process releases heat, effectively acting as a heat source within the porous medium. This heat release influences both the temperature distribution and the heat transfer processes. As a result, the heat variation term in the heat transfer model for porous media can be expressed as follows:

$$Q = m_h \Delta H_D - \varphi\rho S_g \sigma_g \frac{\dot{\partial} p_g}{\partial t} - \rho_g v_g \cdot \sigma_g \nabla p_g \tag{8}$$

$$\Delta H_D = \begin{cases} 215.59 \times 10^3 - 394.945T, & 248K < T < 273K \\ 446.12 \times 10^3 - 132.638T, & 273K < T < 298K \end{cases} \tag{9}$$

Where $\sigma_g$ is the joule Thomson coefficient, $\mathrm{J/(kg \cdot Pa)}$; $p_g$ is the gas Pressure, Pa; $\Delta H_D$ is the endothermic rate of hydrate decomposition (Selim and Sloan, 1989), $\mathrm{W/m^3}$.

### 2.3.3 *Hydrate formation model in porous media*

During the gas–water two-phase flow in porous media, hydrate formation begins at the gas–water interface once the temperature and pressure conditions necessary for hydrate formation are met. This process is essentially the reverse of hydrate decomposition. Using the kinetic model for hydrate formation introduced by Kim et al. (1987), the rate of hydrate formation in porous media is determined through the following equation:

$$m_{hf} = kA_a(p - p_e) \tag{10}$$

In this equation, $m_{hf}$ represents the hydrate formation rate, measured in mol/s; $A_a$ denotes the gas–water contact surface area in $m^2$; $k$ is the hydrate formation rate constant, which differs from the constant used for hydrate decomposition. The value of $k$ is $5.9\times10^{-12}$ mol/($m^2$·Pa·s) as Sun and Mohanty (2006) determined. Finally, $p - p_e$ refers to the driving force for hydrate formation, measured in Pascals (Pa). To model the formation of hydrates in porous media, a theoretical approach was developed to calculate the surface area involved in hydrate formation, $A_a$, as proposed by Sun and Mohanty (2006). This model accounts for how much the pore surface area participates in the hydrate formation process. The calculation of $A_a$ is expressed using the following equation:

$$A_a = \Gamma A_p \tag{11}$$

$A_p$ represents the pore surface area per unit volume, measured in $m^{-1}$. This includes both the exposed surface of the porous media and the particle surfaces created during hydrate formation. The parameter Γ denotes the fraction of the pore surface area actively participating in the hydrate formation process and is dimensionless. The pore surface area per unit volume ($A_p$) in porous media can be calculated using the following equation:

$$A_p = \sqrt{\frac{\varphi_{wg}^3}{2K}} \tag{12}$$

The percentage of the pore surface area participating in hydrate formation, Γ, can be determined using the following equation, as proposed by Sun and Mohanty (2006):

$$\Gamma = [S_g S_w (S_h + S_{ie})]^{2/3} \tag{13}$$

$$S_g + S_w + S_h = 1 \tag{14}$$

In this equation, $S_{ie}$ represents the volume fraction of ice, which is dimensionless. During the process of hydrate decomposition, when the local temperature in the porous media falls below freezing, a portion of the free water may transform into solid ice. This results in the presence of a certain volume fraction of ice during the reformation of hydrates. If no ice phase is present during hydrate formation, the equation simplifies and can be expressed as:

$$\Gamma = (S_g S_w S_h)^{2/3} \tag{15}$$

It is important to note that the above formula is no longer valid when $S_h = 0$, where $S_h$ represents the hydrate saturation. To simulate hydrate formation under conditions where $S_h = 0$, it is assumed that $S_h = 10^{-3}$ when its value is less than $10^{-3}$ (Sun and Mohanty, 2006). This assumption ensures the model can account for the initial stages of hydrate formation. Therefore, the hydrates formed are considered to be deposited in situ, creating a hydrate deposition layer. In this process, the hydrate deposition rate in porous media is assumed to equal the hydrate formation rate. This relationship is expressed through the following equation:

$$m_{hd} = m_{hf} = k\sqrt{\frac{\varphi_{wg}^3}{2K}}[S_g S_w (S_h + S_{ie})]^{2/3}(p - p_e) \tag{16}$$

Based on the above-established model, the hydrate formation and deposition rates under gas-water two-phase flow conditions in porous media can be calculated. These calculations enable the determination of hydrate saturation and the progression of the hydrate formation process, including developing hydrate flow obstacles. Furthermore, according to the chemical equation governing hydrate formation, the consumption rates of $CO_2$ and water during the process can be expressed as follows:

$$m_g = -m_{hf}\frac{M_g}{N_h M_w + M_g} \tag{17}$$

$$m_w = -m_{hf}\frac{N_h M_g}{N_h M_w + M_g} \tag{18}$$

Table 1. Properties and operational conditions

| | Parameters | Value |
|---|---|---|
| Aquifer | Thickness, H(m) | 15 |
| | Intrinsic permeability, K ($m^2$) | $1\times10^{-13}$ |
| | Porosity, ∅ | 0.3 |
| $CO_2$ | Viscosity, $\mu_n$ (Pa· s) | $3.95\times10^{-5}$ |
| Brine | Density, $\rho_w$ (kg· $m^{-3}$) | 1045 |
| | Viscosity, $\mu_w$ (Pa· s) | $2.54\times10^{-4}$ |
| Hydrate | Hydrate number, $N_h$ | 6 |
| | Formation kinetic constant, $k_f$ (kg· $m^{-2}$ · $Pa^{-1}$ · $s^{-1}$) | $2.59\times10^{-13}$ |
| | Density, $\rho_h$ (kg· $m^{-3}$) | 910 |
| | Heat capacity, $C_{ph}$ | 2220 |
| Operation | Injection rate, $u_0$ ($m^3$ · $day^{-1}$) | 1600 |

### 2.4 *Results and discussion*

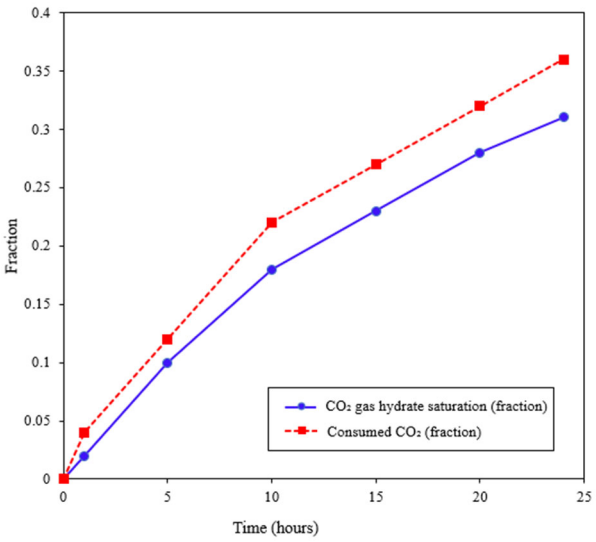


Figure 2. Consumed $CO_2$ and $CO_2$ gas hydrate formed

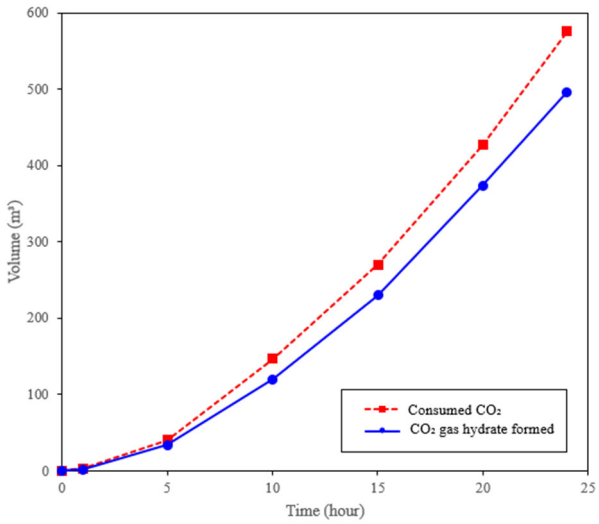


Figure 3. $CO_2$ gas hydrate saturation and $CO_2$ consumed (fractional representation)

In this study, $CO_2$ was injected at a rate of 1600 m³/day for 24 hours to simulate gas hydrate formation. The results were analyzed to evaluate $CO_2$ hydrate saturation trends and $CO_2$ consumption efficiency over time.

For the Ulleung Basin, gas hydrates keep forming due to favorable temperature and pressure conditions (Figure 4). As shown in Figure 2, $CO_2$ consumption increases rapidly during the initial 5 hours, reaching a fraction of 0.12. However, hydrate saturation lags behind, reaching only 0.10. This behavior highlights the delay in hydrate nucleation and formation efficiency. By 24 hours, hydrate saturation stabilizes at 0.31, while $CO_2$ consumption reaches 0.36, indicating a conversion efficiency of approximately 86%. Figure 3 shows the total amount of gas consumption and the amount of gas hydrate formation during injection. The gas of absolute quantities also reveals a consistent gap between $CO_2$ consumed and hydrate saturation throughout the simulation. By 24 hours, the total $CO_2$ consumed is 576 m³, and $CO_2$ hydrate saturation reaches 496 m³. The consistent gap of ~80 m³ indicates unconverted $CO_2$, indicating that not all injected $CO_2$ immediately converts into hydrate, likely due to dissolution effects and kinetic delays in nucleation and crystal growth. The conversion efficiency of $CO_2$ into hydrate gradually improves, reaching a maximum of 87.4% at 20 hours. This improvement corresponds to favorable conditions for hydrate growth as the system stabilizes. However, the presence of unconverted $CO_2$ suggests kinetic limitations and transport resistance within the sediment. The formation of gas hydrates is an exothermic reaction, releasing heat into the surrounding environment and causing a localized increase in temperature (Figure 6). Figure 7 illustrates how pressure evolves over time during the formation of gas hydrates. As gas hydrates develop within the pore spaces, the medium's permeability significantly decreases, slowing pressure change propagation. The results show a continuous increase in pressure near the injection point and a gradual stabilization of the pressure gradient between the injection site and the surrounding areas. This stabilization occurs due to the reduced permeability, which restricts further fluid flow. The pressure dissipation profile exhibits an asymmetrical pattern, with a more rapid decay observed toward the upper boundary of the domain. This behavior is linked to the upward migration of water, driven by the hydrostatic pressure at the top boundary. As a result, the upper region experiences quicker pressure dissipation compared to lateral directions. Additionally, the pressure distribution is more localized than temperature changes, as indicated by the smaller spatial range of pressure variations. This difference underscores the dominant role of permeability in controlling pressure propagation during hydrate formation.

A simulation of gas hydrate formation was also conducted for the Jeju Basin to compare its suitability with the Ulleung Basin. The results showed no hydrate formation in the Jeju Basin over time. Gas hydrate saturation remained at 0.001, the initial value set to avoid computational errors (Figure 5).

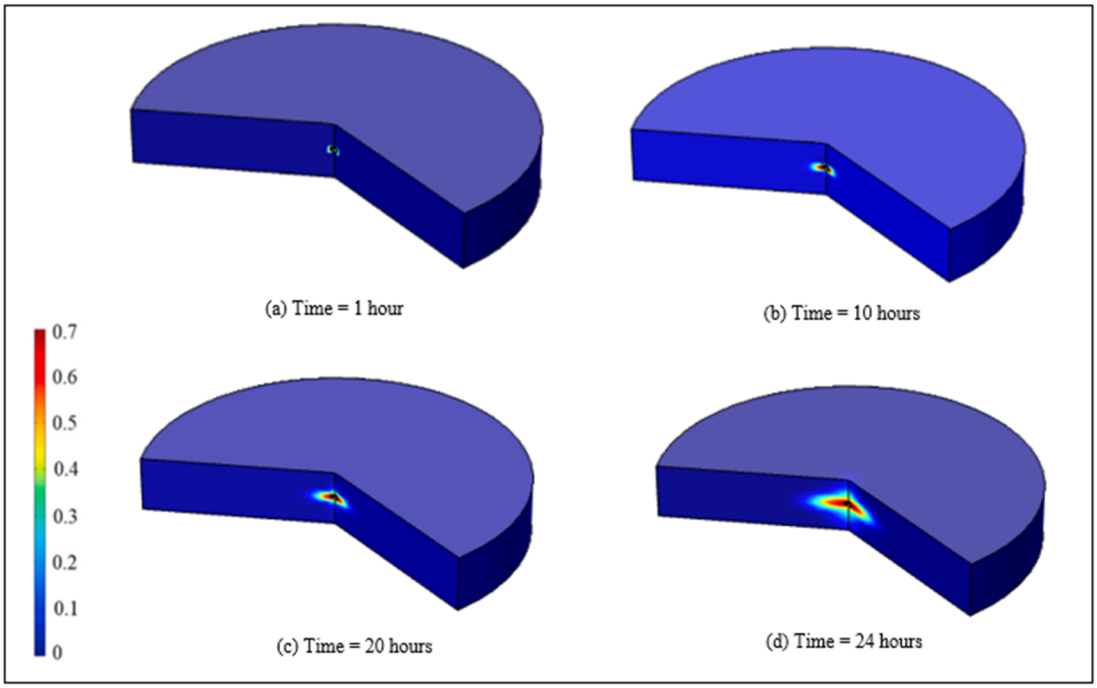


Figure 4. Gas hydrate saturation distribution (a) 1 hour, (b) 10 hours, (c) 20 hours, (d) 24 hours (Ulleung Basin)

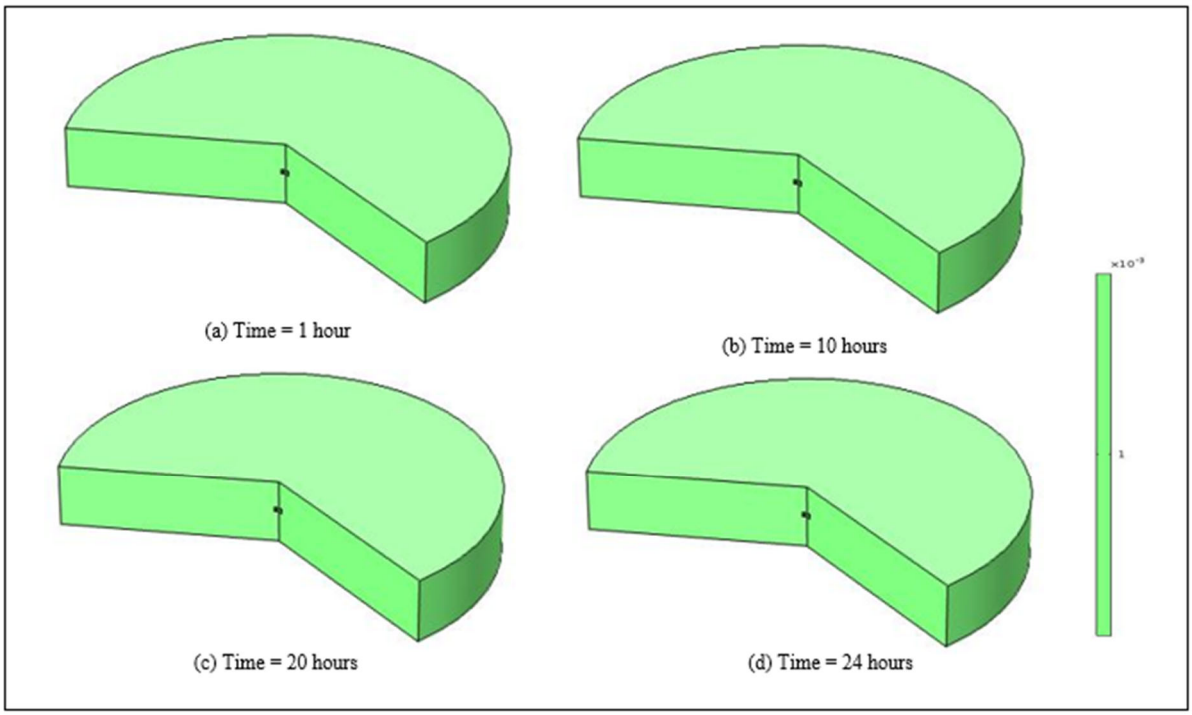


Figure 5. Gas hydrate saturation distribution (a) 1 hour, (b) 10 hours, (c) 20 hours, (d) 24 hours (Jeju Basin)

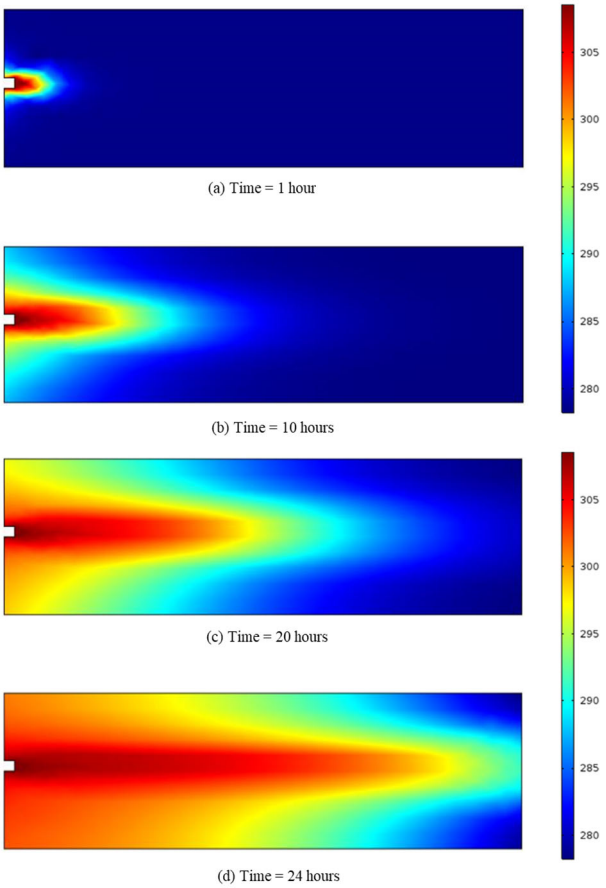


Figure 6. Temperature distribution while gas hydrate formation (a) 1 hour, (b) 10 hours, (c) 20 hours, (d) 24 hours (Ulleung Basin)

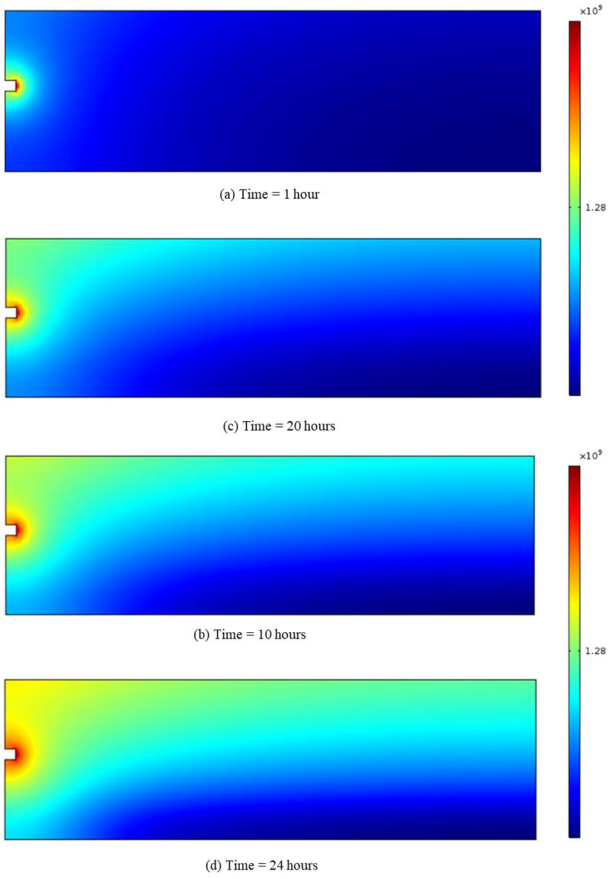


Figure 7. Pressure distribution while gas hydrate formation (a) 1 hour, (b) 10 hours, (c) 20 hours, (d) 24 hours (Ulleung Basin)

## 3 CONCLUSION

This study numerically investigated the coupled processes of $CO_2$ injection, hydrate formation, and fluid displacement in porous marine sediments to assess the feasibility of geological carbon storage via hydrate formation. Using a modified kinetic model integrated with a thermal energy balance equation in COMSOL Multiphysics, we evaluated how pressure–temperature (P–T) conditions, injection parameters, and site characteristics influence hydrate growth and $CO_2$ conversion efficiency. Results for the Ulleung Basin demonstrated continuous hydrate formation under favorable P–T conditions, achieving a maximum $CO_2$ conversion efficiency of 87.4% after 20 hours and maintaining approximately 86% after 24 hours of injection. The simulation revealed that hydrate nucleation and growth exhibit kinetic delays, leading to unconverted $CO_2$ and a consistent saturation gap between consumed gas and hydrate volume. The exothermic nature of hydrate formation caused localized temperature increases, while reduced permeability from hydrate accumulation significantly influenced pressure distribution, producing an asymmetrical dissipation pattern. In contrast, the Jeju Basin exhibited no hydrate formation, highlighting the critical role of site-specific P–T stability zones in determining feasibility. The findings confirm that $CO_2$ storage via hydrate formation is a viable and efficient approach when implemented in geologically suitable offshore sites. This research contributes to the broader understanding of hydrate-based carbon sequestration by quantifying formation kinetics, thermal effects, and permeability impacts, thereby providing valuable insights for optimizing injection strategies and site selection in marine sediment environments.

## 4 ACKNOWLEDGEMENTS

This work was supported by the National Research Foundation of Korea (NRF) grant funded by the Korea government. (MSIT) (2023R1A2C300559611)

## 5 REFERENCES

Bachu, S. (2003) 'Sequestration of $CO_2$ in geological media in response to climate change', *Environmental Geology*, 44(3), pp. 277–289.

Bybee, K. (2006) '$CO_2$ storage in natural-gas-hydrate reservoirs benefits from associated methane production', *Journal of Petroleum Technology*, 58(6), pp. 65–67.

Deng, X., Zhu, Y., Sun, L., Yuan, Q., Li, X. and Chen, G. (2020) 'An improved model for the migration of fluids caused by hydrate dissociation in porous media', *Journal of Petroleum Science and Engineering*, 188, 106876.

Handa, Y.P. (1986) 'Compositions, enthalpies of dissociation, and heat capacities in the range 85 to 270 K for clathrate hydrates of methane, ethane, and propane, and enthalpy of dissociation of isobutane hydrate, as determined by a heat-flow calorimeter', *Journal of Chemical Thermodynamics*, 18(9), pp. 915–921.

Keenan, T.F. and Williams, C.A. (2018) 'The terrestrial carbon sink', *Annual Review of Environment and Resources*, 43(1), pp. 219–243.

Kim, H.C., Bishnoi, P.R., Heidaryan, E. and Kalogerakis, N. (1987) 'Kinetics of methane hydrate decomposition', *Chemical Engineering Science*, 42(7), pp. 1645–1653.

Miocic, J.M. et al. (2016) 'Controls on $CO_2$ storage security in natural reservoirs and implications for $CO_2$ storage site selection', *International Journal of Greenhouse Gas Control*, 51, pp. 118–125.

Mwakipunda, G.C., Abelly, E.N., Mgimba, M.M., Ngata, M.R., Nyakilla, E.E. and Yu, L. (2023) 'Critical review on carbon dioxide sequestration potentiality in methane hydrate reservoirs via $CO_2$–$CH_4$ exchange: Experiments, simulations, and pilot test applications', *Energy & Fuels*, 37(15), pp. 10843–10868.

Selim, M.S. and Sloan, E.D. (1989) 'Heat and mass transfer during the dissociation of hydrates in porous media', *AIChE Journal*, 35(6), pp. 1049–1052.

Sun, X. and Mohanty, K.K. (2006) 'Kinetic simulation of methane hydrate formation and dissociation in porous media', *Chemical Engineering Science*, 61(11), pp. 3476–3495.

Zheng, J., Chong, Z.R., Qureshi, M.F. and Linga, P. (2020) 'Carbon dioxide sequestration via gas hydrates: a potential pathway toward decarbonization', *Energy & Fuels*, 34(9), pp. 10529–10546.